

Anomalous Diffusion in Plasma Turbulence Models

B. A. Carreras 1), V. E. Lynch 1), L. Garcia 2), G. M. Zaslavsky 3)

1) Oak Ridge National Laboratory, Oak Ridge, Tennessee, U.S.A.

2) Universidad Carlos III, Madrid, Spain

3) Courant Institute of Mathematical Sciences, New York University, New York, New York

e-mail contact of main author: carrerasba@ornl.gov

Abstract. To explore the character of the underlying transport in plasma turbulence, we have followed the motion of pseudo-particle tracers during the nonlinear evolution of three-dimensional turbulence models. These calculations have been performed for three different turbulence models and are associated with resistive interchange, resistive ballooning, and i modes, respectively. The finite-scale Lyapunov number is used to determine the anomalous diffusion exponent. The numerical results for these three models show that the transport mechanism is superdiffusive with an anomalous diffusion exponent in the range (0.85, 0.92).

1. Introduction

Purely diffusive transport processes cannot explain a variety of transport experiments in magnetically confined plasmas. Two examples of such experimental results are scaling of the confinement time in L-mode plasmas [1] and perturbative experiments [2-4]. Self-similarity properties of the probability distribution plasma edge function of fluctuations and turbulent fluxes indicate that the turbulent fluctuations are non-Gaussian [5,6]. All of these experimental results undermine the transport picture based only on the standard diffusion mechanisms.

There are many possible mechanisms in plasmas that can lead to anomalous diffusion. The existence of coherent structures, avalanche type processes, and streamers may significantly change the character of transport. Here, we use conventional plasma turbulence models based on three different types of instabilities to investigate induced transport properties. These models are: 1) the three-dimensional (3-D) pressure-gradient-driven turbulence model in cylindrical geometry [7] where the underlying instabilities are resistive interchange modes; 2) the 3-D pressure-gradient-driven turbulence model in toroidal geometry [8] where the underlying instabilities are resistive ballooning modes; and 3) the 3-D ion temperature-gradient-driven turbulence model [9] where the underlying instabilities are i modes. In these studies it is essential to carry out the calculations over a broad range of space and time scales. The coupling of processes on these different scales is essential in identifying anomalous diffusion processes.

For these models, we have followed the motion of tracer pseudo-particles and evaluated the finite-scale Lyapunov number [10] as a way of determining the transport exponent γ . For a

Research sponsored by the Office of Fusion Energy, U.S. Department of Energy, under contract DE-AC05-00OR22725 with UT-Battelle, LLC

normal diffusion process, $\alpha = 1/2$. All calculations presented here lead to transport exponents of $\alpha > 1/2$, indicating that all of them are superdiffusive.

The rest of this paper is organized as follows. In Sect. 2, we introduce the pseudo-particle tracers and discuss the method of evaluating the exponent α . The numerical results are summarized in Sect. 3. Finally, the conclusions of this work are given in Sect. 4.

2. Pseudo-Particle Tracers in Steady-State Turbulence

The three turbulence models used in the present calculations have already been studied in detail [7-9]. Because of limited space, rather than describe these models we refer readers to these references for detailed explanations. The underlying instabilities for the three models are driven by a gradient, either the pressure gradient or the ion temperature gradient. Therefore, for the three models there is a similar coupling between gradient evolution and turbulence. Changes in the gradient trigger local instabilities in the plasma at the corresponding resonance surface. The instability locally flattens the pressure profile and causes an increase of the gradient in the nearby surfaces. Because of this increase, they may become unstable, and so the process repeats itself in the near singular surfaces. This mechanism causes a propagation of unstable behavior across all or parts of the plasma. Eventually, the excess pressure deposited at the core is transported to the edge of the plasma. This process has the characteristic properties of an avalanche. It is a true avalanche in the sense that there is propagation both up and down the gradient. The downward propagation is, in general, dominant.

To study the transport properties of these three models, we use pseudo-particles as tracers. These tracers are solutions of the equation of motion:

$$\frac{d\vec{r}}{dt} = \vec{V}(\vec{r}, t) = \frac{1}{B^2} \vec{E} \times \vec{B} = \frac{1}{B^2} \nabla \psi(\vec{r}, t) \times \vec{B}. \quad (1)$$

Here, the velocity is the $E \times B$ velocity, because there are no diamagnetic effects included in these models, and is given in terms of the stream function. The three models are electrostatic; therefore, all information on turbulence evolution is through the electrostatic potential (stream function) ψ .

To investigate the dynamics, we have followed orbits of tracer particles. In their evolution, the tracer particles are either trapped in eddies for times that may be long compared with the eddy turnover time or they can jump over several sets of eddies in a single flight. These jumps are normally triggered by the correlated growth of adjacent eddies, as described previously. Therefore, both characteristic features of the anomalous diffusion, trapping and flights, are present in these models. Section 3 describes how we can evaluate the trapping times. However, from a quantitative point of view, we have found no simple way of defining and evaluating particle flights.

In following the tracer orbits, we have calculated the ensemble average of several powers of the radial displacement as a function of time. As discussed in Refs. [11,12], because of the finite size of the system, one can evaluate different moments of the distribution function of the radial positions of the tracer particle to extract the proper similarity exponent. That is, we calculate $\langle [r(t) - r(0)]^n \rangle = D_0 t^{n \alpha(n)}$, where $r(t) = |\vec{r}(t)|$. Here, the angle brackets indicate ensemble averaged over the particle tracers. We can evaluate these moments for different

values of n . Moments with $n < 1$ give the relevant value of α . From this calculation, we can determine whether the diffusion is normal, $\alpha = 0.5$, or anomalous, $\alpha > 0.5$.

We found [12] that it is more accurate to use an alternative approach [10] to determine the exponent α . Following the method of Ref. [10], we initialize a bunch of N particles and define an initial mean square separation between them as

$$\langle r^2(0) \rangle = \frac{1}{N} \sum_{i=1}^N \left| r_i(0)^2 - \langle r_i(0) \rangle^2 \right|, \quad (2)$$

where $\langle r_i(0) \rangle$ is the mean radial position of the bunch of tracer particles. We follow M bunches of N particles and determine for each bunch the time, $T_j(1)$, taken to increase by a factor of λ their initial mean square separation, that is, to have a mean square separation of $\langle r^2(1) \rangle = \lambda \langle r^2(0) \rangle$. The mean time to increase by a factor of λ the mean separation between

particles is then $\langle T_j(1) \rangle = (1/M) \sum_{j=1}^M T_j(1)$. This experiment can be repeated by successive increases by a factor of λ of the mean square separation between particles. After m iterations, the particles will have a mean square separation of $\langle r^2(m) \rangle = \lambda^m \langle r^2(0) \rangle$, with the average time taken to reach this state being $\langle T_j(m) \rangle$. This allows us to define a finite-scale Lyapunov exponent of

$$[\alpha(\lambda, m)] = \frac{\ln(\lambda)}{\langle T_j(m) \rangle}. \quad (3)$$

For $\lambda > 0$, Eq. (3) gives the standard Lyapunov exponent. A plot of α as a function of λ has three well-defined regions. At very low values of λ , α is independent of λ . In this region, α is the Lyapunov exponent. The second region shows a power fall off, $\alpha(\lambda) \sim \lambda^{-1/\nu}$. Here, the exponent ν is the scaling exponent we are looking for. In the third region, α falls off fast. This last region corresponds to particles walking out of the system.

3. Numerical Results

The turbulence calculations are performed over a radial region on the order of 30 to 50 eddy widths. This size of the turbulence region allows us to have a separation of scales such that λ has an algebraic range over one decade. For each determination of α , we have followed an average of 15 bunches of 2000 particles each. The time evolution required for this determination is about 200 eddy turnover times.

In Fig. 1, we have plotted α for the three turbulence models. For more than a decade of values of λ , α is well described by a power law. The calculated exponents for these three cases are close to each other and are given in Table I. They are all greater than 0.5; this indicates that the transport process is superdiffusive.

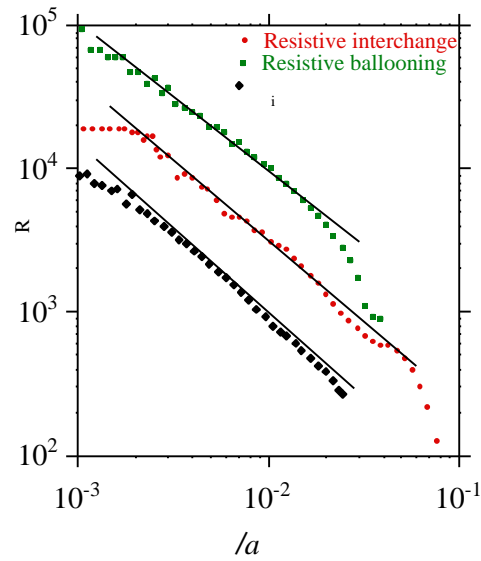


FIG. 1. The finite-scale Lyapunov number R as a function of $/a$ for the three different turbulence models listed in Table I.

TABLE I

Turbulence model	
Pressure-gradient-driven turbulence (interchange)	0.87
Pressure-gradient-driven turbulence (ballooning)	0.88
Ion temperature-gradient-driven turbulence	0.92

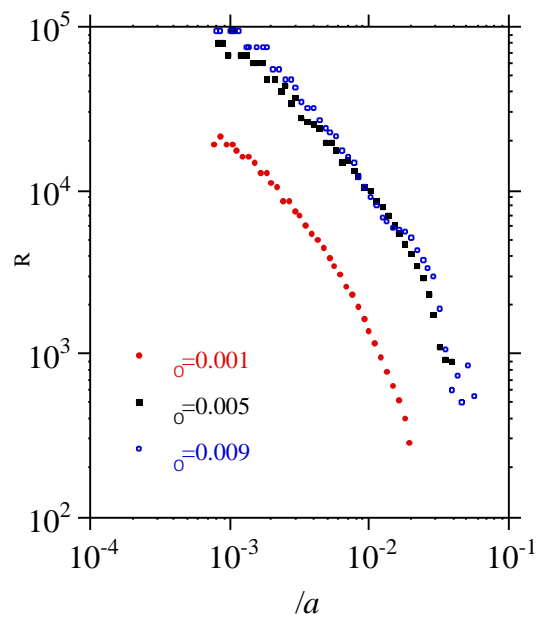


FIG. 2. The finite-scale Lyapunov number R as a function of $/a$ for three values of σ_0 in the case of resistive ballooning-induced turbulence.

We have explored different conditions for these turbulence models and have found very little change on the value of the exponents. For the resistive interchange model, these different conditions are discussed in Ref. [12]. Here, as an illustration, we discuss the case of the resistive ballooning turbulence. In this case, the main parameter use in varying the turbulence conditions is β_0 .

In Fig. 2, we have plotted β_0 as a function of β for three different values of β_0 . For the lowest value, the turbulence spectrum is dominated by a single coherent mode. This case corresponds to the transition regime from stable plasmas to fully developed turbulence [13]. In this case, it is difficult to find a well-established algebraic scaling region. If it exists, it is less than a decade in β . However, for the other two values of β_0 , well into the turbulence region there is a broad region of algebraic scaling. For both values of β_0 , the scaling exponent β_0 has similar value. The $\beta_0 = 0.005$ case has a somewhat higher value of β_0 , close to 1. For $\beta_0 = 0.009$, the value of β_0 is given in Table I.

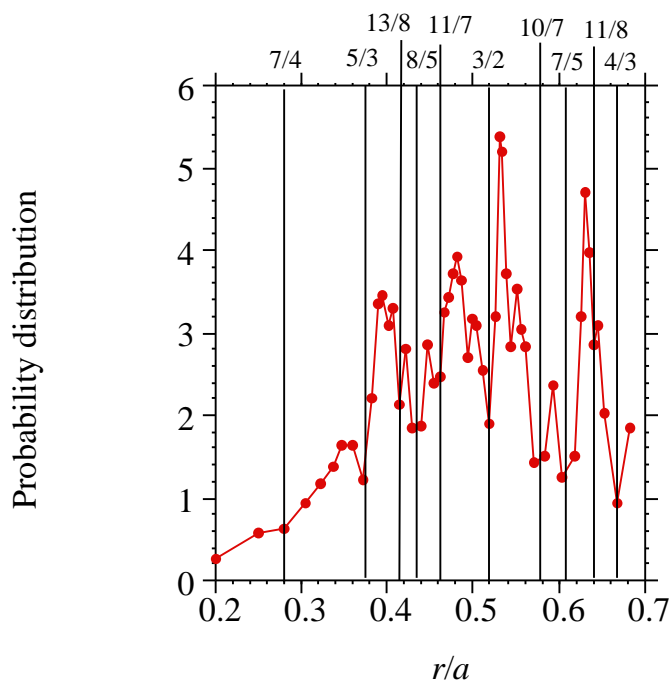


FIG. 3. Probability distribution function of the radial positions where two particles that started close together separate for the resistive interchange turbulence model. We have used a requirement of 100 events per bin to minimize noise. In this figure, we have also plotted the positions of the low rational surfaces.

The transport picture from these calculations agrees with the one put forward in Ref. [14]. Particles are trapped in eddies at the resonant surfaces; they move as jets along the torus. When the particles reach near the boundary of the eddy, where the trajectories become stochastic, they travel fast radially and can travel across several eddies in a single flight. This combination of trapping and flights is consistent with the simple transport picture based on the continuous random walk formalism [15] and given by the sandpile model of Ref. [11].

To better understand this picture, we can evaluate the trapping times at different positions in the plasma column. Let us consider a particle trajectory that we call basic trajectory, and a second trajectory that starts simultaneously with the first one. The initial condition for the second trajectory differs from the basic one by a small distance δ_0 . When the distance $\delta(t)$ between the two trajectories reaches a given value, δ_f , we measure and store the time, T , such that $\delta(T) = \delta_f$. At this point, we start a new trajectory for the same basic trajectory, and we repeat the process. After many iterations, we accumulate a sequence of times that it takes the trajectories to get δ_f apart. We also accumulate the information on the radial position where they separate. This approach is similar to the usual method of determining the Lyapunov number but for a finite size separation. In the following results, we have used $\delta_0 = 0.001a$, the lowest possible value, because of the limitation of the radial resolution, and $\delta_f = 0.003a$.

We have evaluated the radial distribution of the separation position of the particles. This distribution is radially nonuniform. For the resistive interchange turbulence, the minima of the distribution are clearly associated with low m and n resonant surfaces (Fig. 3). In this case, the vortex structures are uniform toroidally and it is in the region between eddies where separation occurs. If we look at the position of minimum T , that is, maximum finite size Lyapunov numbers, they are uniformly distributed poloidally and around the hyperbolic points of the stream function. In this case, the cause of stochastization of the orbits is in the time behavior of these eddies and bursts of particles are associated with the correlated dynamical evolution that we can interpret as avalanches.

In the case of the resistive ballooning turbulence, the situation is more complicated. At low values, when we are in the transition regime from stable to fully developed turbulence, a single mode dominates the spectrum. In this case, and as shown in Fig. 4 for $\delta_0 = 0.001$, the minima of the probability distribution function of the separation points are correlated with the singular surfaces where the different poloidal components of this mode are resonant. We can see this in Fig. 4 for the $n = 23$ mode. However, the poloidal distribution of the separation point is nonuniform. Eddies associated with different resonant surfaces in the outer region of the plasma tend to coalesce, and they appear as a radially elongated structures [16]. However, as we move toroidally, these eddies shrink and this structure separates in different eddies that twist around the torus with slightly different pitch. This causes poloidal and radial spreading of eddies that is maximal in the inner region of the torus. In that region, there is a multiplicity of hyperbolic points for the stream function and the separation points with low T values cluster there while they are nearly absent in the outer region of the torus. In this system, the inverse of T can no longer be identified with a finite-size Lyapunov number. This complex vortex structure by itself may lead to radial transport without need of chaotic behavior of the orbits. Both vortex structure and dynamics may be involved in causing particle bursts.

For values in the fully developed turbulence regime, there is no clear way of associating the minima of the probability distribution function of the separation points with rational surfaces. An example of probability distribution of separation points for $\delta_0 = 0.005$ is shown in Fig. 5. As δ_0 increases, there is a tendency towards a more uniform poloidal distribution of the separation points, although a certain level of in-out asymmetry always exists. In this case, the separation between transport induced by structures and by dynamical processes may be more difficult to distinguish.

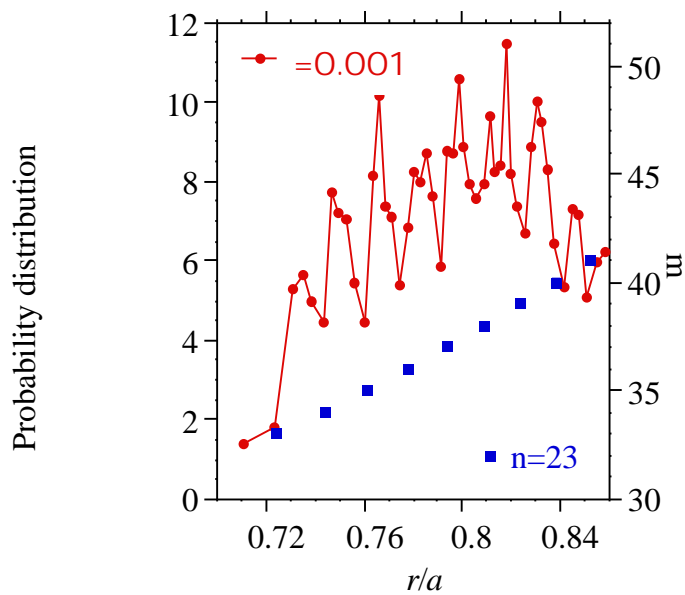


FIG. 4. Probability distribution function of the radial positions where two particles that started close together separate for the resistive ballooning turbulence model with $\nu_0 = 0.001$. In this figure, we have also plotted the positions of the rational surfaces associated with the $n = 23$ mode.

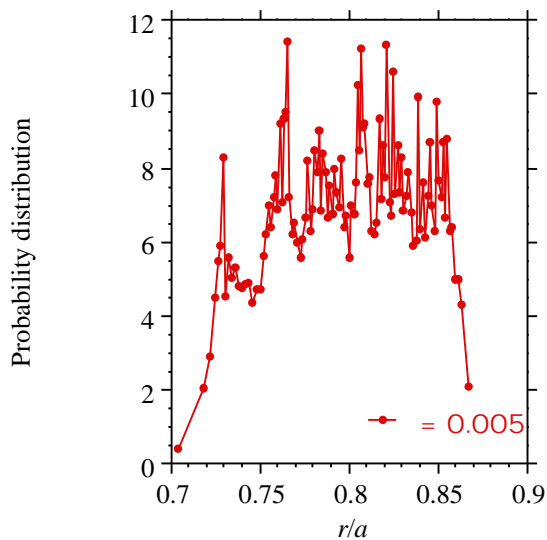


FIG. 5. Probability distribution function of the radial positions where two particles that started close together separate for the resistive ballooning turbulence model with $\nu_0 = 0.005$.

4. Conclusions

Transport of tracer particles in three different plasma turbulence models in the fully turbulence regime indicates that the transport mechanism is superdiffusive. The transport exponents calculated from the finite-scale Lyapunov method gives similar values for the three models and they are around 0.9.

Although the values of the exponent are similar for the three models considered, the mechanism leading to anomalous diffusion may be different. Understanding the space-time structures linked to the different models is essential in defining experiments that may clarify the basic transport mechanism.

Determination of the exponent is important for constructing plasma transport models that incorporate the multiplicity of timescales involved in transport. The transport dynamics of the tracer particles may be interpreted with fractional kinetics [17], as discussed in Ref. [12]. This interpretation provides a consistent picture of the trapping time distributions and the radial anomalous diffusion exponent.

References

- [1] GOLDSTONE, R.J., “Energy confinement scaling in tokamaks: Some implications of recent experiments with ohmic and strong auxiliary heating”, *Plasma Phys. Controlled Fusion* **26** (1984) 87.
- [2] GENTLE, K., et al., “The evidence for nonlocal transport in TEXT”, *Phys. Plasmas* **4** (1997) 3599.
- [3] CALLEN, J.D., et al., “Evidence and concepts for non-local transport”, *Plasma Phys. Control. Fusion* **39** (1997) B173.
- [4] JACCHIA, A., et al., “Nonlocal diffusivity: Impact on transient transport studies”, *Phys. Plasmas* **2** (1995) 4589.
- [5] CARRERAS, B.A., et al., “Self-Similar Regimes and Probability Distribution Function of Turbulence-Induced Particle Fluxes”, *Phys. Rev. Lett.* **83** (1999) 3653.
- [6] ZASLAVSKY, G.M., et al., “Large Scale Behavior of the Tokamak Density Fluctuations”, *Phys. Plasmas* **7** (2000) 3691.
- [7] CARRERAS, B.A., et al., “A Model Realization of Self-Organized Criticality for Plasma Confinement”, *Phys. Plasmas* **3** (1996) 2903.
- [8] GARCIA, L., et al., “Effect of Poloidally Asymmetric Sheared Flow on Resistive Ballooning Turbulence”, *Phys Plasmas* **6** (1999) 3910
- [9] LEBOEUF, J.N., et al., “Full-Torus Landau Fluid Calculations of Ion Temperature Gradient-Driven Turbulence in Cylindrical Geometry”, *Phys Plasmas* **7**, (2000) 5013.
- [10] ARTALE, V., et al., “Dispersion of passive tracers in closed basins: Beyond the diffusion coefficient”, *Phys. Fluids* **9** (1997) 3162.
- [11] CARRERAS, B.A., et al., “Anomalous Diffusion in a Running Sandpile Model”, *Phys. Rev. E* **60** (1999) 4770.
- [12] CARRERAS, B.A., et al., “Anomalous diffusion and exit time distribution of particle tracers in plasma turbulence model”, *Phys. Plasmas* **8** (2001) 5096.
- [13] GARCIA, L., et al., “Resistive pressure-gradient-driven instabilities in the transition regime to fully developed turbulence”, *Phys. Plasmas* **9** (2002) 47.
- [14] NEWMAN, D.E., et al., “The Dynamics of Marginality and Self-Organized Criticality as a Paradigm for Turbulent Transport,” *Phys. Plasmas* **3** (1996) 1858.
- [15] MONTROLL, E.W., et al., in *Studies in Statistical Mechanics*, edited by J. Lebowitz and E. Montroll (North-Holland, Amsterdam, 1984) Vol. 11, p. 1.
- [16] BEYER, P. et al., “Streamers and zonal flows in tokamak edge turbulence,” Paper P5.111 28th EPS Conference on Controlled Fusion and Plasma Physics, Madeira, Portugal, June 2001.
- [17] ZASLAVSKY, G.M., “Fractional kinetic equation for Hamiltonian chaos”, *Physica D* **76**, 110 (1994).